RESEARCH ARTICLE

American Journal of Botany

Botanical Society of America
leading scientists and educators since 1893

Interspecific anatomical differences result in similar highly flexible stems in Bignoniaceae lianas

Caian S. Gerolamo[1,4], Anselmo Nogueira[2], Marcelo R. Pace[3], and Veronica Angyalossy[1]

Manuscript received 28 February 2020; revision accepted 7 August 2020.

[1] Departamento de Botânica, Universidade de São Paulo, Instituto de Biociências, Rua do Matão, 277, São Paulo-SP 05508-090, Brazil

[2] Universidade Federal do ABC, Centro de Ciências Naturais e Humanas (CCNH), Rua Arcturus, 03, São Bernardo do Campo-SP 09606-070, Brazil

[3] Departamento de Botánica, Universidad Nacional Autónoma de México, Instituto de Biología, Circuito Zona Deportiva s/n de Ciudad Universitaria, Mexico City 04510, Mexico

[4] Author for correspondence (e-mail: caian.gerolamo@usp.br; caiansg@gmail.com)

Citation: Gerolamo. S, C.. S, A. Nogueira, M. Pace, and V. Angyalossy. 2020. Interspecific anatomical differences result in similar highly flexible stems in Bignoniaceae lianas. *American Journal of Botany*. 107(12): 1622–1634.

PREMISE: Lianas are intriguing forest components in the tropics worldwide. They are characterized by thin and flexible stems, which have been related to a unique stem anatomy. Here, we hypothesized that the anatomical diversity of lianas, varying in shapes, proportions, and dimensions of tissues and cell types, would result in different stem bending stiffnesses across species. To test this hypothesis, we chose four abundant liana species of central Amazonia belonging to the monophyletic tribe Bignonieae (Bignoniaceae) and compared their basal stems for their anatomical architectures and bending properties.

METHODS: Measurements of anatomical architecture and bending stiffness (structural Young's modulus) included light microscopy observations and three-point bending tests, which were performed on basal stems of eight individuals from four Bignonieae species. All analyses, including comparisons among species and relationships between stem stiffness and anatomical architecture, were performed using linear models.

RESULTS: Although the anatomical architecture of each species consists of different qualitative and quantitative combinations of both tissues and cell types in basal stems, all species analyzed showed similarly lower bending stiffnesses. This similarity was shown to be directly related to high bark contribution to the second moment of area, vessel area and ray width.

CONCLUSIONS: Similar values of stem bending stiffness were encountered in four liana species analyzed despite their variable anatomical architectures. This pattern provides new evidence of how different quantitative combinations of tissue and cell types in the basal stems of lianas can generate similarly low levels of stiffness in a group of closely related species.

KEY WORDS anatomical architecture; bending stiffness; Bignonieae; cambial variant; forest disturbance; lianescent vascular syndrome; mechanical properties; plant anatomy; wood vines; Young's modulus.

Lianas have evolved at least over 130 times independently during the evolution of woody plants (Gentry, 1991; Angyalossy et al., 2015), and they are one of the most essential and intriguing forest components in the tropics worldwide (Schnitzer et al., 2015). Under forest disturbances, such as the formation of canopy gaps, the abundance of lianas escalates rapidly (Schnitzer and Carson, 2010). This pattern has been explained by a combination of efficient growth in high-light environments (Baars and Kelly, 1996) and the capacity of lianas to survive and resprout after canopy falls (Putz and Holbrook, 1991; Rowe and Speck, 2015; Rocha et al., 2020). The latter has been related to the unique stem anatomy of lianas, which is characterized by a highly flexible stem, often with abundant parenchymatous tissue that helps resist and quickly repair damage after injuries (Fisher and Ewers, 1991; Rowe et al., 2004; Read and Stokes, 2006).

Liana woods commonly have a similar anatomy that consists of a combination of wide and narrow vessels closely associated (i.e., vessel dimorphism), very wide and tall rays, few fibers, and typically abundant axial parenchyma. Also, liana stems often vary in their cambial activity, resulting in vascular cambial variants (Schenck, 1893; Metcalf and Chalk, 1950; Carlquist, 1981, 1991; Chery et al., 2020). These vascular cambial variants create an incredible and vast array of stem anatomical architectures, such as

stems with phloem wedges, interxylary phloem, or successive cambia (see Carlquist, 1991; Isnard and Silk, 2009; Angyalossy et al., 2012, 2015). What all these cambial variants have in common is the inclusion of soft tissues such as nonlignified axial parenchyma or phloem tissue interspersed with the stiff elements of the stem. These anatomical features have been coined the lianescent vascular syndrome, a noteworthy example of convergent evolution whose features are shared at least in part by all lianas across different plant lineages, even in ferns and monocots (Angyalossy et al., 2015).

Lianas also share a marked ontogenetic shift in their stems. When they first grow, they typically form a dense wood with narrow, infrequent vessels and many fibers, herein termed self-supporting xylem stage. However, as the liana grows, the wood shifts sometimes abruptly to that of the lianescent vascular syndrome described before (Carlquist, 1985; Caballé, 1986, 1993; Ewers et al., 1991). Functionally, young liana stems act as searchers that circumnutate, locating supports and are, therefore, stiffer than older, attached stems. After support is reached, however, the more typical liana wood is attained, and stem stiffness drops dramatically (Speck, 1991, 1994; Rowe et al., 2004; Menard et al., 2009; Isnard et al., 2012). Both stem stiffness and flexibility result from a complex interaction between the arrangement, proportions, and dimensions of the tissues and cell types that make up the stem structure (Niklas, 1992). Since anatomical structure changes throughout liana stem development, each region of the plant has a different bending stiffness (Speck, 1991; Gallenmüller et al., 2004; Chen et al., 2014; Rowe and Speck, 2015).

The relationship between liana bending stiffness and stem anatomy has been traditionally investigated by comparing plants of different habits or evaluating different developmental stages, in general, from the apex to the stem base. In basal stems, lianas are more flexible, twisting, bending, and stretching under tension, commonly surviving even in the case of branch swaying or mechanical accidents such as treefalls (Rowe and Speck, 2015; Rowe, 2018; Rocha et al., 2020). Different patterns of flexibility and resistance in the basal stems are expected to be found among lianescent species as a result of the anatomical diversity of each species (Rowe and Speck, 2015). On the other hand, this anatomical diversity likely characterizes alternative functional designs to attain approximately equal competencies (Marks and Lechowicz, 2006).

In this study, we investigated the structure–function relationship in the basal stems of lianas, exploring in detail both the anatomical architecture and stem bending stiffness in four Amazonian liana species belonging to the tribe Bignonieae (Bignoniaceae). Anatomical architecture was defined herein as a visible expression of the arrangement, dimension, and quantity of anatomical features (Tomlinson, 1987, with modifications). The anatomical regions considered here include bark (periderm, cortex remnants, and secondary phloem), secondary xylem (wood) and pith, and the abundance of cell types in the secondary xylem. This approach allowed us to test whether the anatomical diversity of basal liana stems result in different bending stiffness and which anatomical features better predict the variation of stiffness across closely related liana species. We first examined differences in the anatomical features and bending stiffness (structural Young's modulus) of basal stems across species. Afterward, we tested the relationship between stem anatomical features and bending stiffness.

MATERIALS AND METHODS

Study area

Our studied area was the central Amazonian tropical forest Ducke Reserve. The reserve is located 26 km northwest of Manaus in the state of Amazonas, Brazil (2°55′S, 59°59′W) and is managed by the National Institute for Amazonian Research (INPA). The Ducke Forest has a closed canopy 30 to 35 m high with emergent trees up to 55 m in height and a low-lying subforest (Ribeiro et al., 1999). Mean annual temperature is around 26°C, and mean annual rainfall is about 2300 mm with a dry season between July and October when rainfall is generally <100 mm/month (Marques-Filho et al., 1981). Topography and edaphic features vary across the reserve, from lower altitude areas where the soil is sandy to higher areas where the soil is clayey (Mertens, 2004).

Field sampling of four liana species

We selected four liana species of the tribe Bignonieae distributed in the Ducke Reserve with high abundance in different habitats (liana species abundance data available at ppbio.inpa.gov.br/en/home and at forestplots.net; Nogueira et al., 2020; Rocha et al., 2020). Stem anatomy is variable among species of Bignonieae, owing to the presence of a cambial variant in their stems, i.e., xylem furrowed by phloem wedges (Pace et al., 2009, 2015). In our sampling, we included only mature individuals, attached and established upon other plants, that had reached the forest canopy with a basal stem diameter between one and 2.5 cm about 1.30 m above the rooting point.

For each species, we marked and sampled eight individuals distributed within an area of 4 ha, considering each liana that was rooted, but not connected to another stem, to avoid any clonal plant (Schnitzer et al., 2006). One voucher for each species was deposited at the University of São Paulo Herbarium (SPF; acronym according to Thiers, 2017) to represent each group of eight individuals per species: *Adenocalymma validum* (K.Schum.) L.G.Lohmann (*Gerolamo 07*), *Anemopaegma robustum* Bureau & K.Schum. (*Gerolamo 08*), *Bignonia aequinoctialis* L. (*Gerolamo 10*), and *Pachyptera aromatica* (Barb. Rodr.) L.G.Lohmann (*Gerolamo 09*).

For each specimen in the field (32 specimens in total), one straight stem segment approximately 65 cm long with a constant diameter was collected near the base of the stem between the rooting point and about 1.30 m above the rooting point. We checked the arrangement and distribution of tissues on both ends of the segments with a 10× magnifying hand lens to ensure that the anatomical features stay constant along each segment. Finally, we removed a 2-cm-long portion from each segment for the anatomical procedures, and the remaining sample of each stem (around 60 cm) was used in the biomechanical bending test, as further detailed below.

Anatomical procedures and analyses

Each stem sample was fixed in FAA (formaldehyde, acetic acid, and 50% ethanol; Johansen, 1940) and then preserved in 70% alcohol. We performed transverse, longitudinal tangential, and longitudinal radial sections of each sample, following the procedure established by Barbosa et al. (2010, 2018). Sections were double-stained in 1% w/v astra blue and 1% w/v safranin, evidencing cells with cellulose

and those with cellulose and lignin (Bukatsch, 1972, modified by Kraus and Arduin, 1997), and permanent slides were prepared with Canada balsam.

For qualitative analyses of bark (all tissues outside of the vascular cambium), we characterized the shape and quantity of phloem wedges by using four, or multiples of four phloem wedges, as defined by Pace et al. (2009). For secondary xylem, we followed the terminology adopted by the list of anatomical features of secondary xylem, as proposed by the IAWA Committee (1989), although we have not given the full qualitative description of the wood since it was beyond the goal of our study.

For quantitative analysis, the transverse sections of each anatomical slide were scanned in high resolution with the Pannoramic SCAN equipment (3DHISTECH Ltd., São Paulo, SP, Brazil) and analyzed with the Case Viewer version 3.3.6 software (3DHISTECH). For each specimen, we calculated the percentage of the bark area, lianescent xylem (xylem with wide vessels developed in climbing phases), self-supporting xylem (early-formed dense xylem developed in juvenile and allegedly self-supporting phases), and pith relative to the total area of the stem. In lianescent xylem, the percentages of vessels area, fibers, and parenchyma (radial and axial) were quantified using four quadrants of 0.5 mm^2 near the cambium between the phloem wedges. Additionally, the average vessel tangential diameter (μm, VD maximum and VD minimum), vessel frequency (vessels/mm) and fiber wall thickness (μm) of the lianescent xylem were measured in the transverse section following the procedure established by Scholz et al. (2013). The ray width was quantified for each specimen using 20 measurements in transverse section of the lianescent xylem near the cambium between the phloem wedges.

Biomechanical bending tests of basal stems

To estimate liana stem flexibility, we subjected each stem segment to the three-point bending test as described by Vincent (1990) and Rowe and Speck (1996). We used an apparatus developed by C. S. Gerolamo (Appendix S1) inspired by that used by Rowe et al. (2006). The basal stem segments with 60 cm were kept hydrated for a maximum of 4 h before the bending tests, and samples with a tapering percentage higher than 10% were not considered (Rowe et al., 2006).

Previous analyses carried out with sister taxa spanning all the different anatomical architectures described for the family in the tribe Bignonieae (Pace et al., 2009) showed that the shear effect is minimized in the three-point bending test when values of the span-to-depth ratio are higher than 20 for all specimens studied (Appendix S2). Therefore, we standardized the span-to-depth ratio above 22 to minimize the influence of shear on the measured bending as described by Vincent (1990). Each stem segment approximately 60 cm long was placed horizontally on two vertical supports of the bending apparatus, and consecutive weights (up to five) were added manually at the center of the tested segment. After adding each weight, we waited 60 s for the vertical deflection to stabilize before measurements. We spent 30 min to perform the complete test of each segment of liana stem. Therefore, the vertical deflection of the stem was measured with a millimeter ruler and a digital camera (Nikon P510, Manaus, AM, Brazil). We used just the linear part of the force deflection curve before the applied force was sufficient for the stem to deform beyond its elastic properties.

The flexural stiffness (EI; in Nmm^2) of each segment was calculated using the formula $EI = l^3ß/48$, where l is the distance between the two vertical supports (555 mm) where the tested stem segment is supported, and $ß$ is the slope of the best-fitting regression curve of the force (in N) plotted against deflection (mm). Only curves with R^2 of 0.98 and above were accepted. We calculated the axial second moment of area (I; in mm^4) of each segment by approximating the cross-sectional shape of the segments as an ellipse using the formula $I = \pi a^3 b/4$, where a and b represent the radial widths in the direction of the applied force and perpendicular to the force, respectively. Lastly, structural Young's modulus (E; in MNm^{-2}) was calculated as EI/I of each stem segment, according to Rowe et al. (2006). Structural Young's modulus is understood to represent the bending stiffness of a combination of heterogeneous plant tissues in a plant stem independently of both size and geometry of the sample (Speck and Rowe, 1999).

We also estimated the contribution of bark, lianescent xylem, self-supporting xylem, and pith to the second moment of area that describes the spatial distribution of tissues within the cross section regarding the centroid and neutral axis in bending. To perform this analysis, we digitized outlines of each tissue area based on the cross section of stems. We used a macro command provided by Tancrède Almeras (CNRS, Montpellier, France) in the image analysis software OPTIMAS version 6.5 (Media Cybernetics, Silver Spring, MD, USA) to calculate the contribution of tissues to the total second moment of area in each stem. The macro establishes the center of mass for the total cross-sectional area and then calculates I (mm^4) of each tissue area with reference to a theoretical neutral line (centroid and neutral axis in bending). Consequently, the total second moment of area represents the sum of each second moment of area of each tissue. For more details about this calculation, see Speck et al. (1990).

Statistical analyses

To test whether the quantitative descriptors of the anatomical architecture and biomechanics of basal stems differed among species, we used a one-way ANOVA, followed by a post hoc Tukey's HSD multiple comparison test ($P < 0.05$). Besides, we performed a complementary set of analyses using the diameter size variation as a covariate to evaluate whether the size of each segment modifies the distribution of anatomical traits and the mechanical properties of basal stems in the four liana species.

We also explored the variation of quantitative anatomical features among species using principal component analysis (PCA). In the PCA, we considered the contribution of the four tissues to the second moment of area of stem (bark, lianescent xylem, self-supporting xylem, and pith), and the percentage and features of the cell types in the lianescent xylem (percentage of vessel area, parenchyma and fibers, vessel frequency, fiber wall thickness and ray width). The three main PCA axes that explained most of the variation from the original anatomical features were used in the subsequent analyses (Norusis, 1990). To evaluate which anatomical variables better describe the structural Young's modulus, we performed a multiple linear regression with structural Young's modulus as the response variable and the three first PCA axes (PC1, PC2, and PC3) and species identity as explanatory variables.

We used the Shapiro–Wilk and Bartlett tests to evaluate the normality and homogeneity of variance of the response variables and residuals of each model, respectively. All analytical procedures were performed using R version 2.15.1 software (R Core Team,

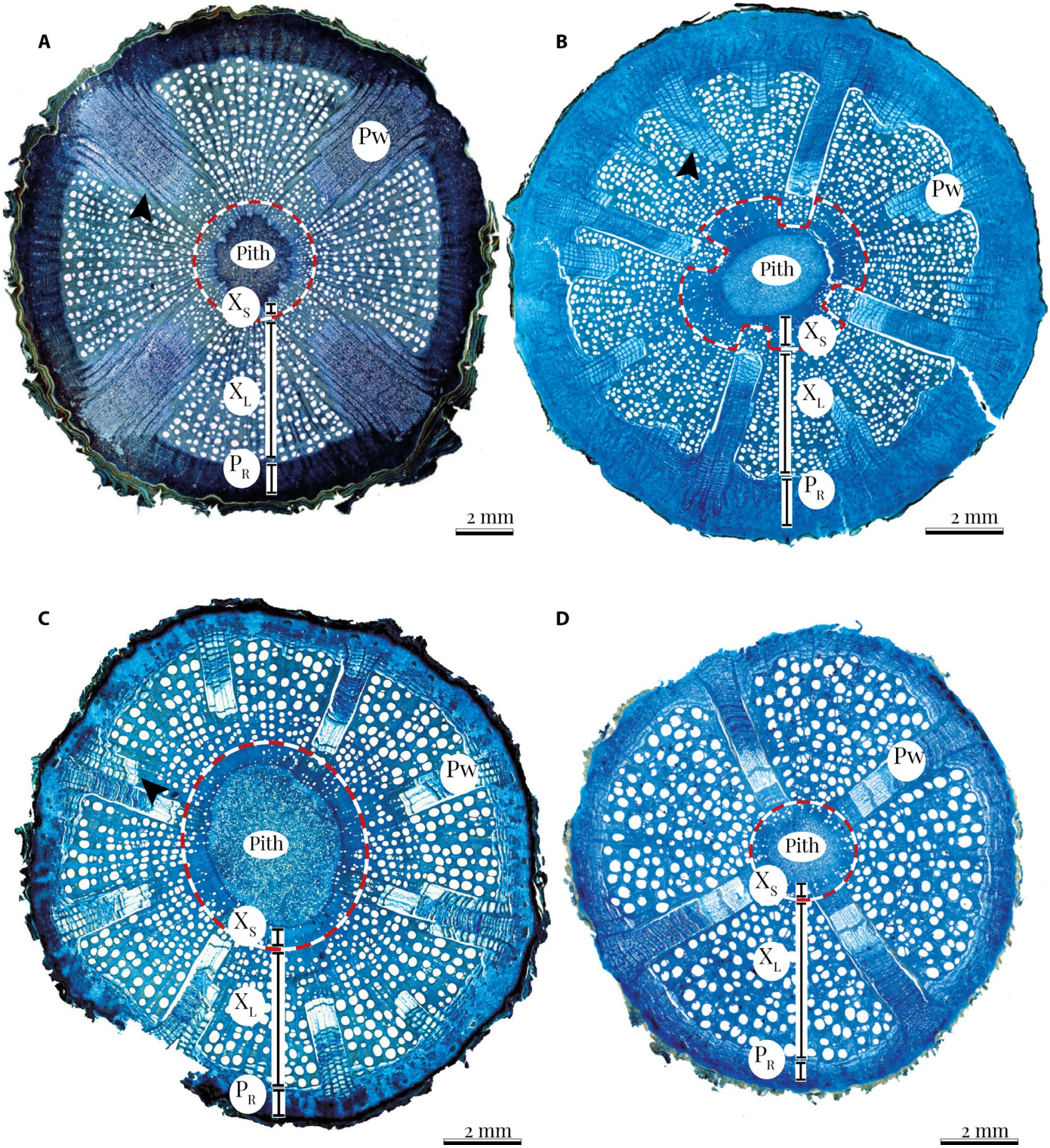

FIGURE 1. Differences in anatomical architecture of basal stems of four species of liana in the Bignonieae. Transverse section of (A) *Adenocalymma validum*, (B) *Anemopaegma robustum*, (C) *Bignonia aequinoctialis*, and (D) *Pachyptera aromatica*. In (A–D), stems have four phloem wedges (P_w) furrowing the xylem. In (B–C), stems have multiples of four phloem wedges furrowing the xylem. All species have a central pith, followed by wood developed during the self-supporting early growth stage (X_S), the lianescent xylem (X_L) occupying most of the stem area and externally the bark, formed by regular phloem (P_R), phloem wedges, cortex remnants, and the periderm. Arrowhead indicating lateral steps in phloem wedges.

2019) with the vegan package (Oksanen et al., 2018) and multcomp (Hothorn et al., 2016).

RESULTS

Characterization of basal stem anatomy of the four Bignonieae species

The overall anatomy of the stems is here described from the stem outside to the inside, from the bark to the pith.

Bark—The outermost part of all barks analyzed was the periderm, which surrounds the entire stem and may be composed of a single periderm or multiple periderms forming a rhytidome. Cortex remnants and pericyclic fibers were observed in some species (Fig. 1B, C) and internal to them lies the secondary phloem. There are two types of secondary phloem in lianas of Bignonieae: regular phloem and variant phloem. Variant phloem is within phloem wedges that furrow the secondary xylem (Fig. 1), while regular phloem is in between the wedges, herein called interwedge zones. *Adenocalymma validum* and *Pachyptera aromatica* develop four phloem wedges (Fig. 1A, D) and the number of phloem wedges stays constant during ontogeny. In comparison, *Anemopaegma robustum* and *Bignonia aequinoctialis* develop multiples of four phloem wedges (Fig. 1B, C). Most species produce lateral steps in the phloem wedges as the stem grows (Fig. 1A–C), except for *Pachyptera aromatica*, where the phloem wedges are straight without lateral steps (Fig. 1D).

Secondary xylem—The secondary xylem of Bignonieae lianas comprises (1) the lianescent xylem and the (2) self-supporting xylem, which is located next to the pith. The lianescent xylem is characterized by growth rings delimited by radially narrow fibers and a narrow band of marginal axial parenchyma (Fig. 2A, C, E, G), diffuse porosity (Figs. 1, 2), vessel dimorphism with wide vessels predominantly solitary associated with narrow vessels in multiples, forming either short radial chains or clusters (Fig. 2A, C, E, G). Axial parenchyma is scanty paratracheal to vasicentric in the four species, forming short confluences and narrow marginal bands (1 to 3 cells wide). The rays are 1 to 3 cells wide in *Anemopaegma robustum* and *Pachyptera aromatica*, 4 to 6 cells wide in *Adenocalymma validum* and *Bignonia aequinoctialis*.

The self-supporting xylem differs from the lianescent xylem. It has growth rings indistinct in *Adenocalymma validum*, *Anemopaegma robustum*, and *Bignonia aequinoctialis*, but distinct in *Pachyptera aromatica*, delimited by radially narrow fibers and a narrow band of marginal axial parenchyma (Fig. 2B, D, F, H). Vessels appear in low frequency (except for *Pachyptera aromatica*), being narrow, solitary, or in multiples of 2 (Fig. 2B, D, F, H). Vessel dimorphism is less marked (Fig. 2B, D, F, H). Axial parenchyma is scanty paratracheal in all species. Rays are narrower with 1 to 2 cells wide (Fig. 2B, D, F, H). The fibers occupy most of the self-supporting xylem.

Interspecific differences in anatomical features and biomechanics of basal stems

The bark and secondary xylem of basal stems differ quantitatively and qualitatively across liana species, with high contribution of both tissues in cross section and to the second moment of area (I) (Table 1). Stem segments of *Adenocalymma validum* had the highest values for bark contribution to I with 64 ± 0.06% (mean ± SD), 10% more than segments of *Pachyptera aromatica* with the lowest values (N_{plants} = 32, $F_{3, 28}$ = 4.95, P = 0.006; Fig. 3A). In contrast, segments of *P. aromatica* had the highest values of lianescent xylem contribution to I with 42 ± 0.05%, 15% more than segments of *Anemopaegma robustum* with the lowest values (N_{plants} = 32, $F_{3, 28}$ = 8.19, P = 0.0004; Fig. 3B). On average, the contribution of self-supporting xylem and pith to I is around 4% and does not differ among species (N_{plants} = 32, $F_{3, 28}$ = 1.58, P = 0.21 and N_{plants} = 32, $F_{3, 28}$ = 1.38, P = 0.26, respectively). We also investigated the potential impact of the diameter size variation on the contribution of the different tissues to I. The diameter size of the basal stems does not explain the contribution of bark and secondary xylem to I (Appendix S3 A, B) but is negatively related to the contribution of pith to I.

The area occupied by vessels in the lianescent xylem is quite similar among species, on average 36 ± 5.4% (N_{plants} = 32, $F_{3, 28}$ = 2.89, P = 0.06; Fig. 3C). The fiber area in the lianescent xylem is about 10% greater in *A. validum*, *A. robustum*, and *P. aromatica* when compared to *Bignonia aequinoctialis* that has on average 29.9 ± 6.1% (N_{plants} = 32, $F_{3, 28}$ = 6.78, P = 0.002; Fig. 3D). On the other hand, the area occupied by axial and ray parenchyma in the lianescent xylem is lower in *Anemopaegma robustum* and *Pachyptera aromatica* when compared to *Bignonia aequinoctialis* (N_{plants} = 32, $F_{3, 28}$ = 8.10, P < 0.001; Fig. 3E). The average vessel diameter differs among species, and it is about 10% higher in *Adenocalymma validum* and *Bignonia aequinoctialis* (N_{plants} = 32, $F_{3, 28}$ = 12.63, P < 0.001; Fig. 3F). In contrast, vessel frequency is about 20% higher in *Anemopaegma robustum* and *Pachyptera aromatica* (N_{plants} = 32, $F_{3, 28}$ = 18.96, P < 0.001; Fig. 3G). Fiber wall thickness in the lianescent xylem differs between species, being thicker in *Adenocalymma validum* than all other species (N_{plants} = 32, $F_{3, 28}$ = 21.70, P < 0.001; Fig. 3H). Ray in the lianescent xylem is about twice higher in *Adenocalymma validum* and *Bignonia aequinoctialis* (N_{plants} = 32, $F_{3, 28}$ = 30.48, P < 0.001; Fig. 3I). The diameter size of the basal stems does not explain the variation of vessel, fiber, and parenchyma area (Appendix S3C–E). However, the diameter size is positively related to the vessel diameter, ray width, and fiber wall thickness (Appendix S3F–I), although it explains around 11% of the variation of these traits across stem segments.

On average, the structural Young's modulus is similar among species (N_{plants} = 32, $F_{3, 28}$ = 1.45, P = 0.28; Fig. 3J), even when we include the diameter size variation as covariate in our analyses (species effect: N_{plants} = 32, $F_{3, 27}$ = 1.81, P = 0.17). In this last case, the diameter size is negatively related to the structural Young's modulus, explaining 12% of its variation (Appendix S3 J). On average, the structural Young's modulus considering all samples is around 1198 ± 556.3 MNm^{-2}, with the median close to 1058 MNm^{-2}. Besides, the second moment of area does not differ among species (N_{plants} = 32, $F_{3, 28}$ = 1.01, P = 0.41), on average with 4081.6 ± 4070.3 mm^4; similarly to the pattern of flexural stiffness across species (N_{plants} = 32, $F_{3, 28}$ = 1.74, P = 0.18) (Table 1).

Relationship between biomechanics and stem anatomy across species

To test the relationship between the structural Young's modulus with the anatomy of the basal stems across liana species, we first described the variation of quantitative anatomical descriptors among species using PCA (see Materials and Methods for

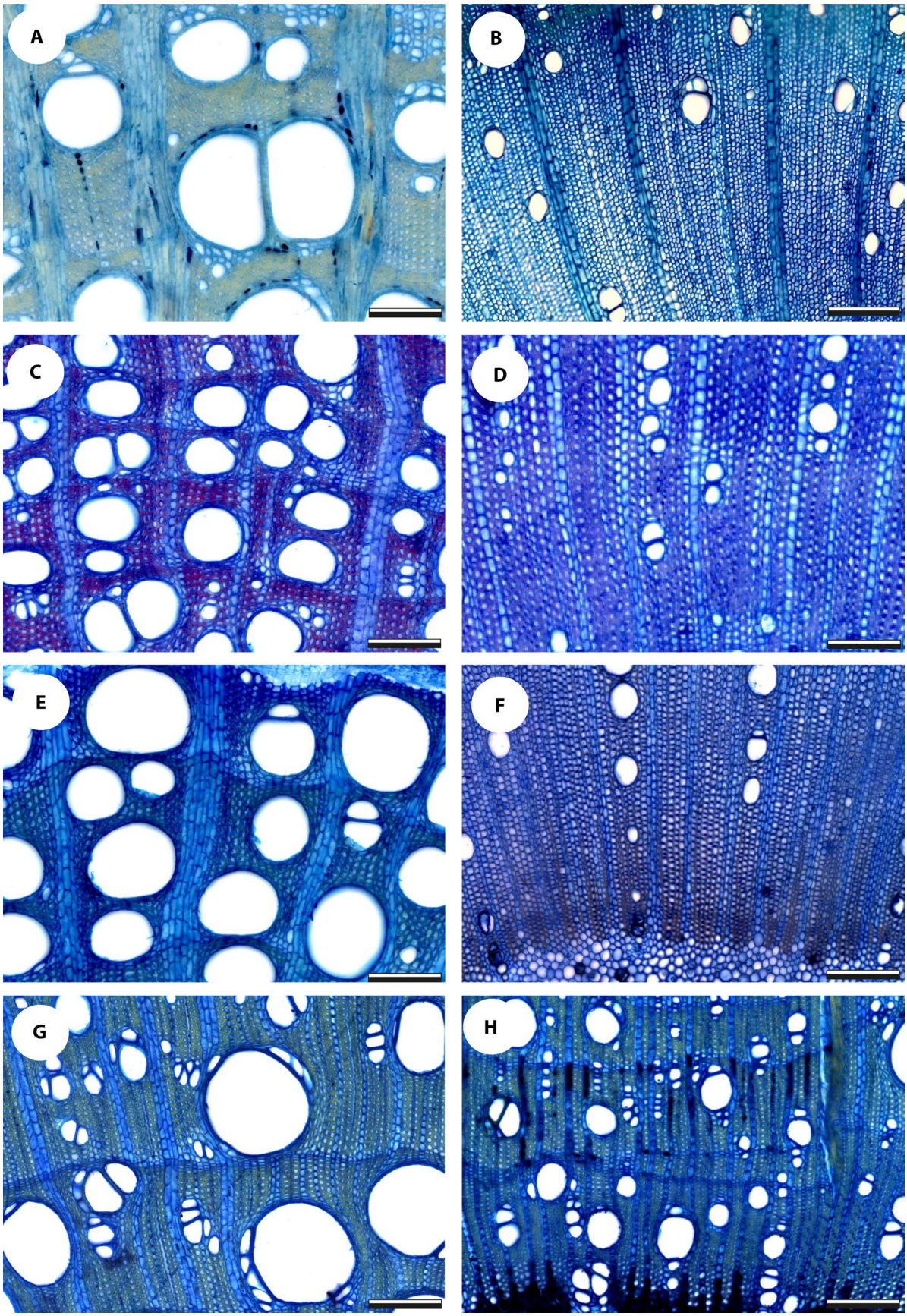
A
B
C
D
E
F
G
H

FIGURE 2. Differences between lianescent xylem and self-supporting xylem in the basal stems in four species of Bignonieae. (A, B) *Adenocalymma validum*, (C, D) *Anemopaegma robustum*, (E, F) *Bignonia aequinoctialis*, (G, H) *Pachyptera aromatica*. In (A), (C), (E), and (G), the lianescent xylem is marked by large areas occupied by very wide vessels associated with clusters of narrow vessels clustered, wide rays, and scanty paratracheal axial parenchyma and narrow marginal bands. In (B), (D), (F), and (H), the self-supporting xylem region is composed of narrow vessels and rays, and most of the area is occupied by fibers. Scale = 200 μm.

details). The proportion of observed variance in the first three axes (PC1, PC2, and PC3) explains 34%, 22%, and 17%, respectively (Fig. 4; Appendix S4). Principal component 1 was positively associated with the self-supporting xylem contribution to *I* and fiber area and negatively associated with the bark contribution to *I*, vessel area, ray width, and fiber wall thickness. Principal component 2 was positively related to the lianescent xylem contribution to *I* and vessel area and negatively associated with the bark contribution to *I*, self-supporting xylem contribution to *I*, and parenchyma area (Fig. 4A). Principal component 3 was positively associated with the bark contribution to *I* and vessel frequency and negatively associated with pith area and parenchyma area (Fig. 4B).

In the regression analysis, PC1 and PC3 had a positive and negative relationship, respectively, with the structural Young's modulus and similar effect size (see b_{st} = standardized slope coefficients below). The lower values of structural Young's modulus (i.e., more flexible stems) were associated with the most negative values of PC1 (Fig. 5A; $N_{plants} = 32$, $b_{st} = 369 \pm 50$, $t_{27} = 7.3$, $P < 0.001$, $R^2_{partial} = 0.67$) that represented stems with a combination of a higher contribution of bark to *I*, vessel area, fiber wall thickness, and ray width, concomitant with a lower contribution of self-supporting xylem to *I* and fiber area. Secondarily, the lower values of structural Young's modulus were associated with the most positive values of PC3 (Fig. 5C; $N_{plants} = 32$, $b_{st} = -309 \pm 52$, $t_{27} = -5.8$, $P = 0.02$, $R^2_{partial} = 0.56$). The positive values of PC3 represented a combination of higher contribution of bark to *I* and vessel frequency and lower contribution of pith to *I* and percentages of the parenchyma area. In the regression analysis, structural Young's modulus also did not differ among liana species ($N_{plants} = 32$, $t_{27} = -0.2$, $P = 0.84$). For additional details of the regression analysis and graphical inspections, circumnutating see the supporting information (Appendix S5–S7).

DISCUSSION

Lianas are a very heterogeneous plant group composed of phylogenetically distant plant lineages sharing a set of common structural features in their stem anatomy (Carlquist, 1985; Angyalossy et al., 2015). This structural similarity of stems is thought to be a convergent evolutionary response to a common hydraulic and mechanical selective pressure, which favors very efficient water conduction and highly flexible, fracture-resistant basal stems (Rowe, 2018). Although we detected striking anatomical differences between the sampled species, all of them exhibited low and similar bending stiffness in basal stem, contrary to our original hypothesis, which expected differences in stem anatomy to reflect in different

TABLE 1. Basal stem anatomical features and mechanical properties (mean ± SD) for each liana species. Descriptive statistics were calculated based on eight individuals per species.

	Adenocalymma validum	*Anemopaegma robustum*	*Bignonia aequinoctialis*	Pachyptera aromatica
Anatomical features				
Cambial variant	4 phloem wedges	Multiples of 4 phloem wedges	Multiples of 4 phloem wedges	4 phloem wedges
Mean diameter stem (mm)	16.17 (±2.95)	15.99 (±3.29)	16.21 (±5.70)	13.47 (±2.50)
Stem area (mm^2)	168.86 (±61.34)	193.60 (±69.56)	173.11 (±100.85)	112.77 (±38.62)
Bark area (%)	44.22 (±5.83)	44.53 (±5.99)	40.93 (±3.34)	35.30 (±5.53)
Xylem area (%)	51.96 (±5.94)	48.78 (±7.90)	50.78 (±4.88)	57.50 (±3.68)
Lianescent xylem area (%)	47.14 (±7.12)	35.31 (±13.78)	40.65 (±13.37)	51.27 (±6.46)
Self-supporting xylem area (%)	6.93 (±6.70)	13.47 (±16.09)	10.13 (±8.99)	6.23 (±3.91)
Pith area (%)	3.80 (±2.07)	6.67 (±5.14)	8.28 (±7.25)	7.18 (±5.21)
Vessel area (%)	37.2 (±4.96)	31.5 (±7.93)	37.1 (±3.96)	37.7 (±5.79)
Parenchyma area (%)	27.6 (±4.11)	26.4 (±5.19)	32.8 (±5.21)	23.0 (±3.42)
Fiber area (%)	35.1 (±5.60)	41.9 (±8.16)	29.9 (±6.06)	39.2 (±6.14)
Fiber wall thickness (μm)	8.48 (±0.59)	7.04 (±0.51)	6.70 (±0.46)	6.68 (±0.49)
Vessel frequency (vessels/mm)	24.25 (±5.00)	46.06 (±14.43)	20.40 (±4.54)	45.37 (±6.80)
Vessel diameter (μm)	48.81 (±4.98)	36.35 (±7.47)	51.49 (±7.51)	39.45 (±2.39)
Minimum and maximum vessel diameter (μm)	13 – 268	13 – 173	15 – 242	12 – 284
Ray width (μm)	80.93 (±14.4)	33.03 (±5.5)	70.28 (±19.4)	32.74 (±6.5)
Mechanical properties				
Bark contribution to *I* (%)	64 (±0.06)	66 (±0.06)	62 (±0.03)	55 (±0.08)
Lianescent xylem contribution to *I* (%)	34 (±0.06)	27 (±0.08)	34 (±0.04)	42 (±0.05)
Self-supporting xylem contribution to *I* (%)	0.72 (±0.69)	6.7 (±10.4)	3.3 (±4.5)	1.9 (±2.7)
Pith contribution to *I* (%)	0.17 (±0.15)	0.27 (±0.2)	0.94 (±1.36)	0.79 (±1.13)
Second moment of area (*I*; mm^4)	4401 (±2828)	4205 (±2642)	5592 (±7144)	2127 (±1802)
Flexural stiffness (*EI*; $MNmm^2$)	3.36 (±2.03)	5.01 (±5.48)	5.01(±5.41)	2.07(±1.69)
Structural Young's modulus (*E*; MNm^{-2})	870.4 (±373)	1340.8 (±494)	1383.4 (±631)	1197.4 (±634)

biomechanical properties. There were multiple possible quantitative combinations of tissues and cell types in the basal stems generating similar biomechanical properties across species. Some anatomical combinations were the best predictor of the lower bending stiffness of the liana stem: the simultaneous occurrence of higher bark area, ray width, vessel area, vessel frequency, lower self-supporting xylem, pith area, and total fiber area. In summary, the different anatomical architectures, regardless of the species, had a set of features that when combined in quantitatively different ways attained virtually the same low bending stiffness for the basal stems.

Anatomical architecture and flexibility of liana basal stems

For more than 100 years, the anatomy of the lianas has been explored, especially for their stems (Darwin, 1875; Schenck, 1893; Pfeiffer, 1926; Carlquist, 1991; Angyalossy et al., 2015). While many features are common to all lianas and treated under the lianescent vascular syndrome concept (Angyalossy et al., 2015), these studies have shown a tremendous diversity of stem anatomical architectures, with different tissue configurations and percentage of cell types. This diversity is very high between lineages but taxonomically constant within them; e.g., different stem architectures derived from cambial variants are a valuable feature to distinguish genera, tribes, and families (Caballé, 1993; Angyalossy et al., 2015). In our case, the four liana species sampled have phloem wedges furrowing the xylem, a synapomorphy of the tribe Bignonieae (Lohmann, 2006; Pace et al., 2009), with species varying in the number of phloem wedges in basal stems (Pace et al., 2009, 2015). Although qualitative differences in stem anatomy of lianas are taxonomically informative (e.g., *Pachyptera* with four phloem wedges and *Anemopaegma* with multiples of four phloem wedges), quantitative differences in tissues and cell types are mostly associated with plant organ functionality.

On a macroscopic scale, quantitative analysis of tissues that make up the stem of many liana species (e.g., *Condylocarpon guianense*, *Aristolochia macrophylla*, *Clematis vitalba*, *Stigmaphyllon ellipticum*) is commonly divided into the bark, lianescent xylem, self-supporting xylem (dense and stiff inner wood) and pith (Caballé, 1986, 1993; Ewers and Fisher, 1989; Speck, 1994). In the four studied species, the self-supporting xylem and the pith contributed less than 6% to the stem second moment of area (*I*). In contrast, lianescent xylem (34%) and bark (62%) contributed on average 94% of the *I*. In studies with other liana species (e.g., *Aristolochia macrophylla*, *Aristolochia asclepiadifolia*), the lianescent xylem contributed to about 20–28% and bark (periderm, cortex, and phloem) to approximately 70–80% to the stem second moment of area (Speck, 1994; Wagner et al., 2012). Although the bark has the most significant contribution to *I*, different values of the contribution of the bark and the lianescent xylem to *I* is found in different species of lianas. The contribution of tissues to *I* is critical because the second moment of area is a geometrical parameter that measures the efficiency of a particular area and position of the cross section in resisting bending forces (Niklas, 1992). However, few studies have quantified the contribution of tissue to stem second moment of area in mature liana species, which makes any generalization untimely.

We investigated the lianescent xylem at the microscopic scale in the four Bignonieae species. In general, lianescent xylem includes a relatively large proportion of the cross-sectional area of vessels with the presence of very wide vessels associated with few fibers and a

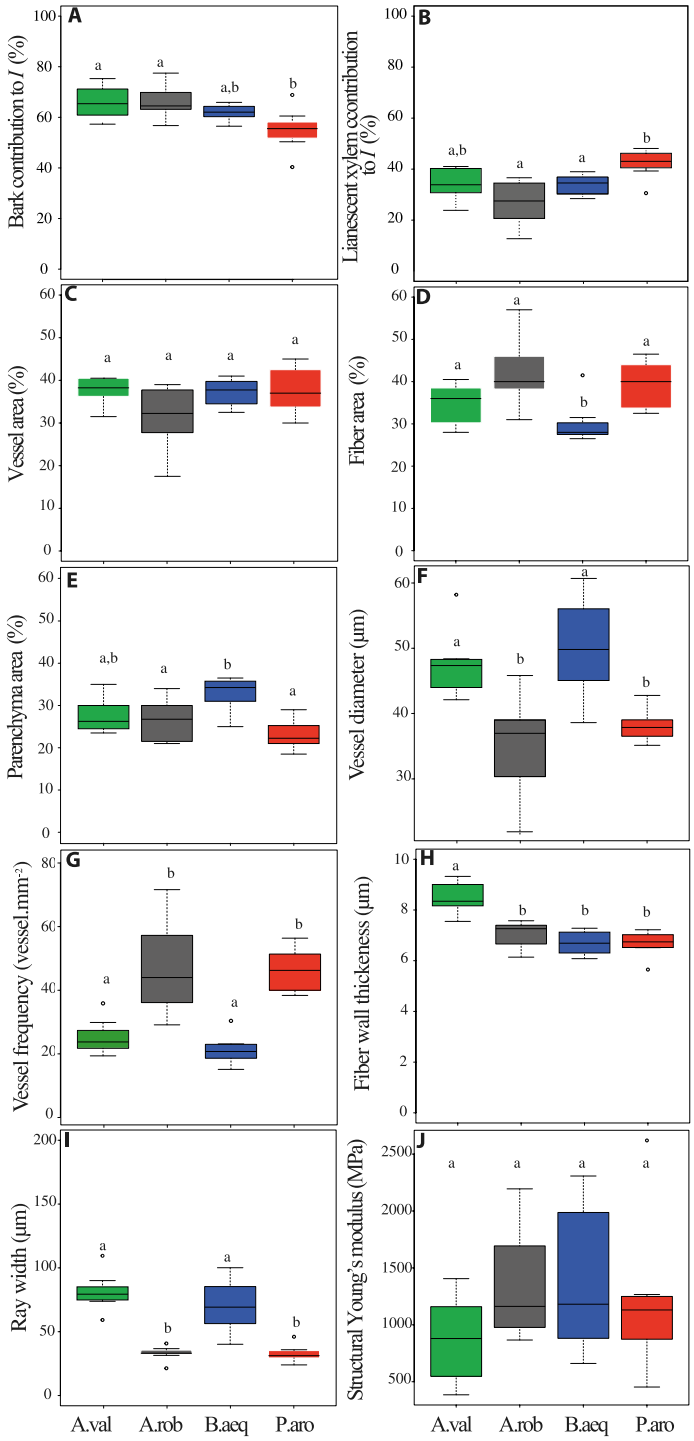

FIGURE 3. Interspecific comparisons of the anatomical structure and Young's modulus of the basal stems in the four Bignonieae species (N = 8 individuals per species). (A–I) Contribution of the tissues to second moment of area (I) and the descriptors of cell types in the lianescent xylem. (J) Structural Young's modulus. A.val = *Adenocalymma validum*, A.rob = *Anemopaegma robustum*, B.aeq = *Bignonia aequinoctiales*, P.aro = *Pachyptera aromatica*. Different letters indicate differences between species based on the post hoc Tukey's HSD multiple comparison test ($P < 0.05$).

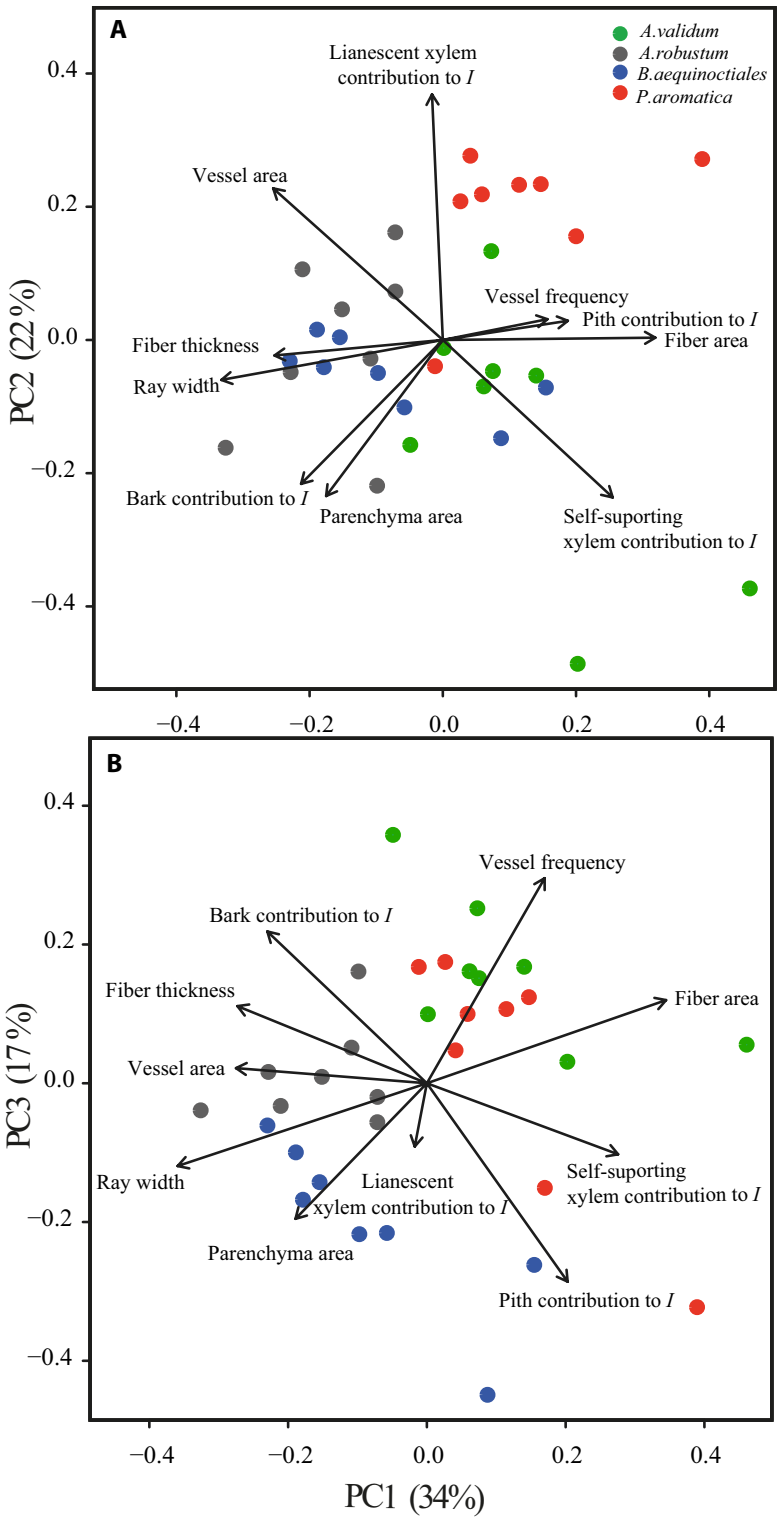

FIGURE 4. Principal component analysis of anatomical features of the basal stems in four Bignonieae species, considering contribution of the tissues to second moment of area (*I*) and the descriptors of cell types in the lianescent xylem according to each species. (A) Relationship between PC1 and PC2. (B) Relationship between PC1 and PC3. PC1, PC2 and PC3 are the first three PCs (proportion of variance). More details about the PCA are available in Appendix S4. Different colors represent stem samples from different Bignonieae species.

high proportion of axial and radial parenchyma and wide and tall rays (Angyalossy et al., 2015). The liana species analyzed here also had these typical anatomical features, except for the proportion of axial parenchyma, which unlike most lianas, occupied only a small area, a feature shared by most lianescent Bignoniaceae species (Gasson and Dobbins, 1991; Pace and Angyalossy, 2013; Pace et al., 2015). At the same time, the four liana species had distinct dimensions and proportions of cell types (vessel, axial and ray parenchyma, and fibers; Fig. 3) composing the lianescent xylem. These different anatomical features in the lianescent xylem, jointly with the variety of tissues, increased the morphological complexity of basal stems of each liana species.

Despite the different anatomical architectures among the four liana species, they had low and similar stem bending stiffnesses, even when we included variations in diameter size into the analyses. The values of the structural Young's modulus found for basal stems in the liana species sampled (average = 1197 MNm^{-2}) were close to those of mature plants of liana species in families such as Euphorbiaceae (*Croton* spp.), Caprifoliaceae (*Lonicera* spp.) and Apocynaceae (*Secamone* spp.) (Gallenmüller et al., 2004; Lahaye et al., 2005; Rowe et al., 2006). The similar stem flexibility of the studied species can be explained by the fact that these lianas have different quantitative combinations of tissues and cell types, forming the different anatomical architectures, but all resulting in similar stem biomechanical properties. This result corroborates the hypothesis of complex interactions among multiple trade-offs, implying that diverse anatomical combinations are feasible in the same habitat, each representing an alternative functional design of approximately equal competence (Marks and Lechowicz, 2006). Besides, the anatomical and structural differences of many plant groups have converged on very similar form–function relationships, as a result of either similar adaptive pressures or because general design constraints underlie the same biological function (Niklas, 1992).

On the other hand, species sampled here were four times less flexible than species of Aristolochiaceae (*Aristolochia* spp.), Convolvulaceae (*Maripa* spp.), and Gnetaceae (*Gnetum* spp.) (Rowe et al., 2006). These lianas have stems showing very wide rays and/or alternation of lianescent xylem, phloem, and conjunctive tissue produced by the activity of successive cambia (Angyalossy et al., 2015). Such anatomical features are directly related to lower bending stiffness of stems (Fisher and Ewers, 1991), and in this case, the anatomical differences appear to be sufficient to change the biomechanical properties of the stem. Although the stem stiffness varies along the stem in response to anatomical change, the lowest stem stiffness is expected to be at the base of the stem in mature lianas reaching the canopy (Speck, 1991; Rowe and Speck, 1996). This portion of the stem has the largest diameter with a higher contribution of the secondary tissues (bark and lianescent xylem). In fact, plant stems are structured by tissues and cell types, being considered a compound material with different mechanical properties, and all tissues or cell types perform functions in

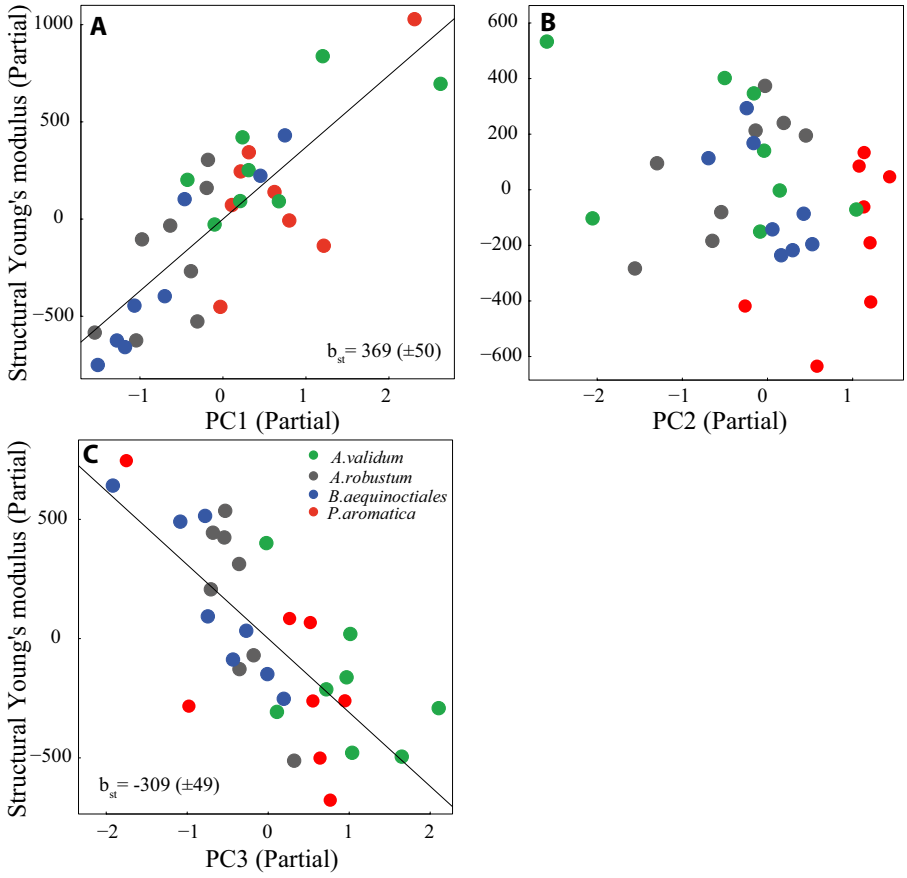

FIGURE 5. Relationships between structural Young's modulus and the three axes of the PCA describing the anatomical variation of the basal stems in the four Bignonieae species. (A) Positive relationship between structural Young's modulus and the PC1 axis. (B) Absence of relationship between structural Young's modulus and the PC2 axis. (C) Negative relationship between structural Young's modulus and the PC3 axis. We also added in each graph the standardized slope coefficients (b_{st} ± SE) describing the size effect of the PCA axes and the structural Young's modulus. Additional details of the statistical model applied in each case are available in Appendix S5. Different colors represent stem samples from different Bignonieae species.

the mechanical structure of the plant (Speck et al., 1990; Niklas, 1992; Baas et al., 2004). How anatomical features of basal stems may contribute or not to the low stem bending stiffness across liana species is further explored below.

Sets of anatomical features associated with higher stem flexibilities in basal stems

In our study, the lower stem bending stiffness was related to the higher contribution of bark to the second moment of area, vessel area, and ray width in the lianescent xylem, combined with a lower contribution of self-supporting xylem and pith to *I*, and fiber area within the lianescent xylem (in our case, concatenated by the PC1 and PC3 axes). These anatomical features form the main set of traits that predict the stem bending stiffness across Bignonieae species. Similarly, in *Condylocarpon guianense* (Apocynaceae) and *Aristolochia macrophylla* (Aristolochiaceae), the increase in phloem and lianescent xylem area during development resulted in a stem with lower bending stiffness (Speck, 1994; Speck and Rowe, 1999). We know that bark structure is composed of soft tissues, such as phloem and cortex remnants (Rowe et al., 2006), while lianescent xylem is often composed of a large area of vessels, a larger amount of parenchyma and wider rays, together forming the compliant liana stems (Rowe et al., 2004).

The contribution of the bark to *I* is the highest, given its peripheral placement in the stem, with phloem wedges furrowing the xylem, clearly influencing the bending properties of the stems. Furthermore, the contribution of the lianescent xylem to *I* is also high, and although it is not directly related to bending properties of the stems in our study, the increase in the area of both vessel and parenchyma (especially ray parenchyma) of the lianescent xylem contributed to lower bending stiffness. All these anatomical features have already been reported to increase stem flexibility in studies comparing liana stages during ontogeny in *Clematis vitalba* (Ranunculaceae), *Aristolochia macrophylla* (Aristolochiaceae), *Condylocarpon guianense* (Apocynaceae), and *Manihot* aff. *quinquepartita* (Euphorbiaceae) (Speck, 1994; Speck and Rowe, 1999; Isnard et al., 2003; Rowe et al., 2004; Menard et al., 2009). In this way, while one species had a more profuse bark (e.g., *Anemopaegma robustum*), other species compensated by having a decreased stem stiffness by the production of wider rays and wider vessels (e.g., *Bignonia aequinoctiales*), both independently contributing to equal increased stem flexibilities.

CONCLUSIONS

Our characterization of the anatomical and biomechanical architecture of the basal stems of four lianas of the tribe Bignonieae showed that different sets of quantitative features generate similar biomechanical properties in the basal stems of these plants. The common pattern of lower values for structural Young's modulus across liana species is indicative of higher stem resistance in response to damage following tree fall events (Read and Stokes, 2006; Rowe, 2018) and guarantees successful climbing and establishment of specimens in the treetops (Isnard and Silk, 2009). Altogether, morphological and biomechanical features contribute to liana survival and abundance under certain ecological conditions (Schnitzer and Carson, 2010; Rocha et al., 2020).

We also evidenced that lower bending stiffness in the basal stem is characterized by a higher contribution of the bark to the second moment of area, and secondarily, by the increase of vessel area and ray width in lianescent xylem. This combination of features in the basal stems of mature lianas should be investigated in other independent lineages of lianas to explore the generality of our observations. Therefore, further studies should combine stem biomechanics, anatomy, and growth dynamic of the lianas to contribute

to the understanding of liana distribution patterns, growth, and survival after disturbances in the tropical forests.

ACKNOWLEDGMENTS

This research was supported by the São Paulo Research Foundation (FAPESP, 2013/10679-0 and 2018/06917-7), Coordenação de Aperfeiçoamento de Pessoal de Nível Superior - Brasil (CAPES, finance code 88882.333016/2019-01), and the Brazilian Long-Term Ecological Research Program (PELD, CNPq Processo 403764/2012-2). We thank L. D. Araujo, F. R. C. Costa and two anonymous reviewers and Associate Editor S. Poppinga for helpful suggestions. We are indebted to Karl Niklas for his comments on our methodology and also thank the C. L. Bastos for assistance with data collection and entire staff of the University of São Paulo, Botany Department (Brazil) and staff of the Department of Reserves (DSER) of the National Institute for Amazonian Research (INPA) for logistical support.

AUTHOR CONTRIBUTIONS

C.S.G., A.N., M.R.P., and V.A. conceived the ideas and experimental design; C.S.G., A.N., and V.A. collected the data; C.S.G. and A.N. identified the plant species. C.S.G. performed anatomical procedures; C.S.G. and V.A. analyzed the anatomical structure; C.S.G. and A.N. analyzed and led the writing of the manuscript. C.S.G., A.N., M.R.P., and V.A. contributed to the writing and approved the final publication.

DATA AVAILABILITY

Data is available online at FigShare (Appendix S8: https://doi.org/10.6084/m9.figshare.12767447.v1).

SUPPORTING INFORMATION

Additional Supporting Information may be found online in the supporting information tab for this article.

APPENDIX S1. Biomechanical apparatus for 3-point bending tests used in this study.

APPENDIX S2. The nonlinear relationship between the structural Young's modulus and the span-to-depth ratio in five liana species spanning the stem anatomical diversity known for member of tribe Bignonieae.

APPENDIX S3. Interspecific comparisons of the anatomical structure and Young's modulus of the basal stems across the four Bignonieae species.

APPENDIX S4. Eigenvalues and loadings of the three first principal components (PC1, PC2, and PC3). Loading were considered significant when the correlations between the anatomical traits and scores PC axes were considered significant after the Bonferroni correction of probabilities (0.05/10 = 0.005) and are highlighted in bold.

APPENDIX S5. Modelling of stem structural Young's modulus, the continuous factors principal components (PC1, PC2, and PC3) and the species referring the anatomical architecture of the stem and the four species as a fixed factor (Young's modulus ~ PC1 + PC2 + PC3 + Species).

APPENDIX S6. Residual analysis and diagnostic for examining the fit of the linear model (structural Young's modulus ~ PC1 + PC2 + PC3 + Species). (A) Plot of residuals against fitted values. (B) Plot of the ordered residuals against the quantiles of the normal distribution.

APPENDIX S7. Relationships between structural Young's modulus and each anatomical variable, including tissue and cell descriptors. b_{st} = standardized slope coefficients different than zero.

LITERATURE CITED

Angyalossy, V., G. Angeles, M. R. Pace, A. C. Lima, C. L. Dias-Leme, L. G. Lohmann, and C. Madero-Vega. 2012. An overview on the anatomy, development and evolution of the vascular system of lianas. *Plant Ecology & Diversity* 5: 167–182.

Angyalossy, V., M. R. Pace, and A. C. Lima. 2015. Liana anatomy: a broad perspective on structural evolution of the vascular system. *In* S. A. Schnitzer, F. Bongers, R. Burnham, and F. E. Putz [eds.], Ecology of lianas, 253–298. Wiley-Blackwell, Oxford, UK.

Baars, R., and D. Kelly. 1996. Survival and growth responses of native and introduced vines in New Zealand to light availability. *New Zealand Journal of Botany* 34: 389–400.

Baas, P., F. W. Ewers, S. D. Davis, and E. A. Wheeler. 2004. Evolution of xylem physiology. *In* A. R. Hemsley and I. Poole [eds.], The evolution of plant physiology, 273–295. Elsevier Academic Press, San Diego, CA, USA.

Barbosa, A. C. F., M. R. Pace, L. Witovisk, and V. Angyalossy. 2010. A new method to obtain good anatomical slides of heterogeneous plant parts. *IAWA Journal* 31: 373–383.

Barbosa, A. C., G. R. Costa, V. Angyalossy, T. C. Dos Santos, and M. R. Pace. 2018. A simple and inexpensive method for sharpening permanent steel knives with sandpaper. *IAWA Journal* 39: 497–503.

Bukatsch, F. 1972. Bermerkungen zur Doppelfarbung Astrablau-Safranin. *Mikrokosmos* 61: 255.

Caballé, G.1986. Sur la biologie des lianes ligneuses en forêt ganonaise. Ph.D. dissertation, Université des Sciences et Technique du Languedoc, Montpellier, France.

Caballé, G. 1993. Liana structure, function and selection: a comparative study of xylem cylinders of tropical rainforest species in Africa and America. *Botanical Journal of the Linnean Society* 113: 41–60.

Carlquist, S. 1981. Wood anatomy of Nepenthaceae. *Bulletin of the Torrey Botanical Club* 108: 324–330.

Carlquist, S. 1985. Observations on functional wood histology of vines and lianas: vessel dimorphism, tracheids, vasicentric tracheids, narrow vessels, and parenchyma. *Aliso: A Journal of Systematic and Evolutionary Botany* 11: 139–157.

Carlquist, S. 1991. Anatomy of vine and liana stems: a review and synthesis. *In* F. E. Putz and H. A. Mooney [eds.], The biology of vines, 53–71. Cambridge University Press, Cambridge, UK.

Chen, Y. J., F. Bongers, J. L. Zhang, J. Y. Liu, and K. F. Cao. 2014. Different biomechanical design and ecophysiological strategies in juveniles of two liana species with contrasting growth habit. *American Journal of Botany* 101: 925–934.

Chery, J. G., M. R. Pace, P. Acevedo-Rodríguez, C. D. Specht, and C. J. Rothfels. 2020. Modifications during early plant development promote the evolution of nature's most complex woods. *Current Biology* 30: 237–244.

Darwin, C. 1875. The movements and habits of climbing plants. J. Murray, London, UK.

Ewers, F. W., and J. B. Fisher. 1989. Variation in vessel length and diameter in stems of six tropical and subtropical lianas. *American Journal of Botany* 76: 1452–1459.

Ewers, F. W., J. B. Fisher, and K. Fichtner. 1991. Water flux and xylem structure in vines. *In* F. E. Putz and H. A. Mooney [eds.], The biology of vines, 127–160. Cambridge University Press, Cambridge, UK.

Fisher, J. B., and F. W. Ewers. 1991. Structural responses to stem injury in vines. *In* F. E. Putz and H. A. Mooney [eds.], The biology of vines, 99–124. Cambridge University Press, Cambridge, UK.

Gallenmüller, F., N. P. Rowe, and T. Speck. 2004. Development and growth form of the neotropical liana *Croton nuntians*: the effect of light and mode of attachment on the biomechanics of the stem. *Journal of Plant Growth Regulation* 23: 83–97.

Gasson, P., and D. R. Dobbins. 1991. Wood anatomy of the Bignoniaceae, with comparison of trees and lianas. *IAWA Bulletin* 12: 389–417.

Gentry, A. H. 1991. The distribution and evolution of climbing plants. *In* F. E. Putz and H. A. Mooney [eds.], The biology of vines, 3–42. Cambridge University Press, Cambridge, UK.

Hothorn, T., F. Bretz, P. Westfall, R. M. Heiberger, A. Schuetzenmeister, S. Scheibe, and M. T. Hothorn. 2016. Package multcomp. Simultaneous inference in general parametric models. Project for Statistical Computing, Vienna, Austria. Website: http://multcomp.r-forge.r-project.org/.

IAWA Committee. 1989. IAWA list of microscopic features for hardwood identification. *IAWA Bulletin* 10: 219–332.

Isnard, S., T. Speck, and N. P. Rowe. 2003. Mechanical architecture and development in *Clematis*: implications for canalized evolution of growth forms. *New Phytologist* 158: 543–559.

Isnard, S., and W. K. Silk. 2009. Moving with climbing plants from Charles Darwin's time into the 21st century. *American Journal of Botany* 96: 1205–1221.

Isnard, S., J. Prosperi, and S. Wanke. 2012. Growth form evolution in Piperales and its relevance for understanding angiosperm diversification: an integrative approach combining plant architecture, anatomy, and biomechanics. *International Journal of Plant Sciences* 173: 610–639.

Johansen, D. A. 1940. Plant microtechnique. McGraw-Hill, New York, NY, USA.

Kraus, J. E., and M. Arduin. 1997. Manual básico de métodos em morfologia vegetal. Editora da Universidade Rural, Rio de Janeiro, Brazil.

Lahaye, R., L. Civeyrel, T. Speck, and N. P. Rowe. 2005. Evolution of shrub-like growth forms in the lianoid subfamily Secamonoideae (Apocynaceae s.l.) of Madagascar: phylogeny, biomechanics, and development. *American Journal of Botany* 92: 1381–1396.

Lohmann, L. G. 2006. Untangling the phylogeny of neotropical lianas (Bignonieae, Bignoniaceae). *American Journal of Botany* 93: 304–318.

Marks, C. O., and M. J. Lechowicz. 2006. Alternative designs and the evolution of functional diversity. *American Naturalist* 167: 55–66.

Marques Filho, A. D. O., H. M. Dos Santos, and J. M. Dos Santos. 1981. Estudos climatológicos da Reserva Florestal Ducke-Manaus, AM, IV-Precipitacao. *Acta Amazonica* 4: 759–768.

Menard, L., D. Mckey, and N. P. Rowe. 2009. Developmental plasticity and biomechanics of treelets and lianas in *Manihot* aff. *quinquepartita* (Euphorbiaceae): a branch-angle climber of French Guiana. *Annals of Botany* 103: 1249–1259.

Mertens, J. 2004. The characterization of selected physical and chemical soil properties of the surface soil layer in the "Reserva Ducke", Manaus, Brazil, with emphasis on their special distribution. Ph.D. dissertation, Humboldt-Universitat zu Berlin, Berlin, Germany.

Metcalfe, C. R., and L. Chalk. 1950. Anatomy of the dicotyledons. Clarendon Press, Oxford, UK.

Niklas, K. J. 1992. Plant biomechanics: an engineering approach to plant form and function. University of Chicago Press, Chicago, IL, USA.

Norusis, M. J. 1990. SPSS/PC+ professional statistics. SPSS, Chicago, IL, USA.

Nogueira, A., F. B. Baccaro, L. Leal, P. J. Rey, L. G. Lohmann, and J. L. Bronstein. 2020. Variation in the production of plant tissues bearing extrafloral nectaries explains temporal patterns of ant attendance in Amazonian understorey plants. *Journal of Ecology* 108: 1578–1591.

Oksanen, J., F. G. Blanchet, M. Friendly, R. Kindt, P. Legendre, D. McGlinn, P. R. Minchin, et al. 2018. Package vegan. Community ecology package, R package version, 2.5-2, 1-296. Website: https://github.com/vegandevs/vegan.

Pace, M. R., and V. Angyalossy. 2013. Wood anatomy and evolution: a case study in the Bignoniaceae. *International Journal of Plant Sciences* 174: 1014–1048.

Pace, M. R., L. G. Lohmann, and V. Angyalossy. 2009. The rise and evolution of the cambial variant in Bignonieae (Bignoniaceae). *Evolution & Development* 11: 465–479.

Pace, M. R., L. G. Lohmann, R. G. Olmstead, and V. Angyalossy. 2015. Wood anatomy of major Bignoniaceae clades. *Plant Systematics and Evolution* 301: 967–995.

Pfeiffer, H. 1926. Das abnorme Dickenwachstum. Handbuch der Pflanzenanatomie. Verlag von Gebrüder Borntraeger, Berlin, Germany.

Putz, F. E., and N. M. Holbrook. 1991. Biomechanical studies of vines. *In* F. E. Putz and H. A. Mooney [eds.], The biology of vines, 73–97. Cambridge University Press, Cambridge, UK.

R Core Team. 2019. R: a language and environment for statistical computing. The R Foundation for Statistical Computing, Vienna, Austria. ISBN 3-900051-07-0. http://www.R-project.org/.

Read, J., and A. Stokes. 2006. Plant biomechanics in an ecological context. *American Journal of Botany* 93: 1546–1565.

Ribeiro, J. E. L. S., M. J. G. Hopkins, A. Vicentini, C. A. Sothers, M. A. S. Costa, J. M. Brito, M. A. D. Souza, et al. 1999. Flora da Reserva Ducke: guia de identificação das plantas vasculares de uma floresta de terra firme na Amazônia Central. National Institute of Amazonian Research [INPA], Manaus, Brazil.

Rocha, E., J. Schietti, C. S. Gerolamo, R. Burnham, and A. Nogueira. 2020. Higher rates of liana regeneration after canopy fall drives species abundance patterns in central Amazonia. *Journal of Ecology* 108: 1311–1321.

Rowe, N. P., S. Isnard, F. Gallenmüller, and T. Speck. 2006. Diversity of mechanical architectures in climbing plants: an ecological perspective. *In* A. Herrel, T. Speck, and N. P. Rowe [eds.], Ecology and biomechanics: a mechanical approach to the ecology of animals and plants, 35–59. Taylor & Francis, Boca Raton, FL, USA.

Rowe, N. P., S. Isnard, and T. Speck. 2004. Diversity of mechanical architectures in climbing plants: an evolutionary perspective. *Journal of Plant Growth and Regulation* 23: 108–128.

Rowe, N. P., and T. Speck. 1996. Biomechanical characteristics of the ontogeny and growth habit of the tropical liana Condylocarpon guianense (Apocynaceae). *International Journal of Plant Sciences* 157: 406–417.

Rowe, N. P., and T. Speck. 2015. Stem biomechanics, strength of attachment, and developmental plasticity of vines and lianas. *In* S. A. Schnitzer, F. Bongers, R. Burnham, and F. E. Putz [eds.], Ecology of lianas, 323–341. Wiley-Blackwell, Oxford, UK.

Rowe, N. P. 2018. Lianas. *Current Biology* 28: R249–R252.

Schenck, H.1893. Beiträge zur Biologie und Anatomie der Lianen im Besonderen der in Brasilien einheimischen Arten. II. Beiträge zur Anatomie der Lianen. *In* A. F. W. Schimper [ed.], Botanische Mittheilungen aus den Tropen. Fisher, Jena, Germany.

Schnitzer, S. A., and W. P. Carson. 2010. Lianas suppress tree regeneration and diversity in treefall gaps. *Ecology Letters* 13: 849–857.

Schnitzer, S., F. Bongers, R. J. Burnham, and F. E. Putz. 2015. Ecology of lianas. Wiley-Blackwell, Oxford, UK.

Schnitzer, S. A., S. J. DeWalt, and J. Chave. 2006. Censusing and measuring lianas: a quantitative comparison of the common methods. *Biotropica* 38: 581–591.

Scholz, A., M. Klepsch, Z. Karimi, and S. Jansen. 2013. How to quantify conduits in wood? *Frontiers in Plant Science* 4: 1–11.

Speck, T. H., H. C. Spatz, and D. Vogellehner. 1990. Contributions to the biomechanics of plants. I. Stabilities of plant stems with strengthening elements of different cross-sections against weight and wind forces. *Botanica Acta* 103: 111–122.

Speck, T. 1991. Changes of the bending mechanics of lianas and self-supporting taxa during ontogeny. *In* Natural structures: Principles, strategies and models in architecture and nature, Proceedings of the II International Symposium Sonderforschungsbereich 230, part I. Mitteilungen des SFB 230 Heft 6, 89–95, Stuttgart, Germany.

Speck, T. 1994. Bending stability of plant stems: Ontogenetical, ecological, and phylogenetical aspects. *Biomimetics* 2: 109–128.

Speck, T., and N. P. Rowe. 1999. A quantitative approach for analytically defining size, growth form and habit in living and fossil plants. *In* M. H. Kurmann and A. R. Hemsley [eds.], The evolution of plant architecture, 447–479. Royal Botanic Gardens, Kew, UK.

Thiers, B. 2017. Index herbariorum: a global directory of public herbaria and associated staff. New York Botanical Garden, Bronx, NY, USA.

Tomlinson, P. B. 1987. Architecture of tropical plants. *Annual Review of Ecology and Systematics* 18: 1–21.

Vincent, J. F. V. 1990. Structural biomaterials, revised ed. Princeton University Press, Princeton, NJ, USA.

Wagner, S. T., S. Isnard, N. P. Rowe, M. S. Samain, C. Neinhuis, and S. Wanke. 2012. Escaping the lianoid habit: evolution of shrub-like growth forms in *Aristolochia* subgenus *Isotrema* (Aristolochiaceae). *American Journal of Botany* 99: 1609–1629.